

# Ground state of the impurity Anderson model revisited: A projector operator solution

P. Roura-Bas<sup>1,1</sup>, I. J. Hamad<sup>2</sup>, and E. V. Anda<sup>3</sup>

<sup>1</sup> Depto de Física CAC-CNEA and Consejo Nacional de Investigaciones Científicas y Técnicas, CONICET, Buenos Aires, Argentina

<sup>2</sup> Consejo Nacional de Investigaciones Científicas y Técnicas, CONICET, and Universidad Nacional de Rosario, Rosario, Argentina

<sup>3</sup> Pontificia Universidade Católica, Rio de Janeiro, Brazil

Received 5 September 2014, revised 11 November 2014, accepted 13 November 2014

Published online 16 December 2014

**Keywords** Anderson impurity model, Anderson Hamiltonian, Kondo effect, projector operator formalism, ground state

\*Corresponding author: e-mail roura@tandar.cnea.gov.ar, Phone: +54 11 67727096, Fax: +54 11 67727121

By means of a projector operator formalism we study the ground state properties of the Anderson Impurity Hamiltonian. The non-perturbative treatment of the model agrees with the previous one, obtained by Inagaki [Prog. Theor. Phys. **62**, 1441 (1979)] by means of a perturbation expansion with respect to the hybridization term. We go beyond the Inagaki's formalism to the next leading order. It provides a very accurate calculation of the energy spectrum in the total spin  $S_T = 0$  sector and, in particular, the ground state energy in the whole parameter space. For a one body spinless system, the dependence of the ground state energy as a function of the impurity level obtained by this procedure

remarkably agrees with analytical results. For the many body case the occupancy of the impurity as a function of the parameters is studied and it agrees with the corresponding one obtained by using the Bethe ansatz and the Numerical Renormalization Group solution of the Hamiltonian. The magnetization and susceptibility of the impurity is analyzed by studying the response of the system to an external magnetic field, from which it is possible to extract the Kondo temperature. The dependence of the Kondo scale with the parameters of the model is in excellent agreement with well-known results.

© 2014 WILEY-VCH Verlag GmbH & Co. KGaA, Weinheim

**1 Introduction** The Anderson impurity model (AIM) [1] has received large attention in the last decades. In the spin fluctuating regime it is equivalent to the Kondo Hamiltonian [2], capable of explaining the behavior of the resistivity as a function of temperature of metals doped with 3d transition metal or 4f rare earth impurities. Furthermore, this Hamiltonian has been on the base of the heavy fermion physics. As the Hubbard Hamiltonian in infinite dimensions can be transformed into a self-consistent renormalized one impurity Anderson Hamiltonian, within the dynamical mean field theory (DMFT) [3] this model has permitted as well the study of several aspects of many-body physics as, for instance, the metal non-metal transition taking place in various systems. More recently the Kondo effect has received great attention associated to the many-body properties of highly correlated electronic nanosystem, as quantum dots or structures of quantum dots [4, 5]. The model has been exactly solved by using the Bethe ansatz formalism [6, 7]. Furthermore, the solution has also been found by a variety of

different numerical approaches as it is the case of Numerical Renormalization Group (NRG) [8], Logarithmic Discretization Embedded Cluster Approximation (LDECA) [9], and Density Matrix Renormalization Group (DMRG) [10]. Several algebraic methods and approximations were developed to search the solution as, for instance, the slave bosons (SB), the non and one crossing approximations (NCA, OCA) [11–14], the renormalized perturbation theory (RPT) [15, 16] and the local moment approach (LMA) [17, 18], among others. A non-perturbative hybridization expansion of the solution was early developed not only for the static ground state properties [19, 20] but also for the dynamic ones [21].

Although the results obtained by the mentioned numerical approaches are very accurate, the approximated schemes have been extensively used to obtain a rapid scanning of the properties as a function of the model parameters.

The development of new powerful solutions of the AIM, the most paradigmatic highly correlated electron model, is a very active area of research as it is demonstrated by the

publication of several recent papers [23–26]. The possibility of treating complex nanosystems or molecules and correlation in the bulk are the most important motivations that justify these efforts. Within this context, here we extend the treatment used by Inagaki [19] for searching the ground state properties to the next leading order in the perturbation series. With these additional contributions, the derived ground state properties remarkably agree with the corresponding exact ones derived from the Bethe ansatz and NRG approaches. Furthermore, we obtain results not only in the mixed valence regime and in the limit of an infinite bandwidth for the conduction electrons, as it was case in the Inagaki's work, but in the complete parameter space. In addition, we propose an alternative algebraic way to get the system of self-consistent equations.

The formalism reduces the relevant functional space to a projected subspace of the total Hilbert space consisting of one many body function characterized by a ground state Fermi sea of  $N$  particles and an empty impurity.

To study the physics of the AIM operating in this projected subspace, the Hamiltonian has to be renormalized. A self-consistent functional renormalization of this Hamiltonian permits to obtain the ground state properties, the Kondo temperature, and the magnetic susceptibility as a function of the parameters of the system. For a spinless one-body system, where exact analytical results can be obtained, our results show remarkable agreement with them. Within this formalism, the incorporation of the many-body interaction due to the double occupation does not introduce any formal complexity in comparison to the one-body problem. The algebra is essentially the same. For the many body case the results of the method are also in very good agreement with the well-known universal behavior of the Kondo regime.

In view of the accurate results obtained and the small computational effort required to obtain them, (no more than a few minutes on a workstation), the approach could be useful to study more complex situations, as an impurity solver within the spirit of the DMFT approach, to study many-body interactions in the bulk, or to analyze systems of several strongly interacting impurities.

The paper is organized as follows. In Section 2 we introduce the model and the projector operator formalism to solve it. In Section 3 we present and discuss the numerical evaluations of different physical magnitudes. Finally, in Section 4 some conclusions are drawn.

**2 Model and formalism** The Anderson Hamiltonian describes a system in which an interacting level is coupled with a conduction band of electrons,

$$H = \sum_{k\sigma} \epsilon_k n_{k\sigma} + \sum_{\sigma} E_d n_{d\sigma} + U n_{d\uparrow} n_{d\downarrow} + \sum_{k\sigma} V_k d_{\sigma}^{\dagger} c_{k\sigma} + h.c., \quad (1)$$

where  $n_{k\sigma} = c_{k\sigma}^{\dagger} c_{k\sigma}$  is the number operator and  $c_{k\sigma}^{\dagger}$  creates a conduction electron with momentum  $k$  and spin  $\sigma$  in the

conduction band; the operators  $n_{d\sigma} = d_{\sigma}^{\dagger} d_{\sigma}$  and  $d_{\sigma}^{\dagger}$  refer to an electron in the interacting localized impurity state characterized by an energy  $E_d$  and Coulomb repulsion  $U$ . The coupling of this level with the bath is taken into account by the hybridization function given in terms of  $V_k$  by  $\Delta(\omega) \equiv \pi \sum_k V_k^2 \delta(\omega - \epsilon_k)$ .

We are looking for the energy of the ground state,  $E_0$  and the ground wave function,  $|\psi_0\rangle$ , of the system of  $N$ -particles satisfying the eigenvalue equation

$$H|\psi_0\rangle = E|\psi_0\rangle. \quad (2)$$

We define the projector operator  $P_1 = \prod_{k\sigma \leq k_F} n_{k\sigma}$ , where  $k_F$  is the Fermi wave vector and  $P_2 = 1 - P_1$ . The operator  $P_1$  gives a non-zero result only when it acts in the ground state of a  $N$ -electrons Fermi sea. The action of the projectors is then to split the Hilbert space of  $N$ -particles into two disjoint subspaces, namely  $S_1$  which consists of only one state,  $|\phi_1\rangle = \prod_{k\sigma \leq k_F} c_{k\sigma}^{\dagger} |0\rangle$ , the ground state Fermi sea with no electrons in the  $d$ -level and  $S_2$  with  $|\phi_2\rangle$  representing the rest of the states in the Hilbert space.

The renormalized Hamiltonian that operates on the  $S_1$  subspace can be obtained by eliminating  $|\phi_2\rangle$  of the Schrödinger equation (2). The effective Hamiltonian is given by [27]

$$\tilde{H}|\phi_1\rangle = \left( H_{11} + H_{12} \frac{1}{E - H_{22}} H_{21} \right) |\phi_1\rangle = E|\phi_1\rangle, \quad (3)$$

where  $H_{ij} = P_i H P_j$ . The only contribution to the Hamiltonian  $H_{21}$ , that connects the space  $S_1$  to  $S_2$ , comes from the hybridization term in Eq. (1). Its operation destroys an electron of the Fermi sea and promotes it into the impurity generating a singlet state belonging to the  $S_2$  subspace:

$$|\phi_{kd}\rangle = \sum_{\sigma} \frac{d_{\sigma}^{\dagger} c_{k\sigma}}{\sqrt{2}} |\phi_1\rangle, \quad (4)$$

where the factor  $\sqrt{2}$  is included in order to normalize the new state. Here and in what follows, we employ the notation  $k$  and  $K$  for wave numbers below and above the Fermi level respectively. We emphasize that the state  $|\phi_{kd}\rangle$  is, by construction, a singlet  $S_T = 0$  as we discuss below. Applying  $\langle\phi_1|$  to the left of Eq. (3) we obtain an equation for the energy  $E$ :

$$E = \epsilon_T + 2 \frac{V^2}{N} \sum_{k,k'} \langle\phi_{kd}|\frac{1}{E - H_{22}}|\phi_{k'd}\rangle, \quad (5)$$

where  $\epsilon_T = 2 \sum_k \epsilon_k$  represents the energy of the ground state of the Fermi sea. Also, in (5), we neglect the  $k$  dependence of the hopping  $V_k = V/\sqrt{N}$  as usual, where the scaling by  $1/\sqrt{N}$  is necessary to obtain finite contributions to the energy of the Fermi sea-impurity hopping term.

It can be noticed that to get an explicit expression for the eigenvalues in (5), it is sufficient to calculate the matrix elements of the operator  $(E - H_{22})^{-1}$  between the states  $|\phi_{kd}\rangle$  corresponding to a singlet formed between Fermi sea holes of momentum  $k$  and an electron at the impurity. These states

are accessed by only one application of the different  $k$  contributions of the Hamiltonian  $H_{12}$  to  $|\phi_1\rangle$  in the  $S_1$  subspace.

Furthermore, as we create the space  $S_2$  by successive applications of the Hamiltonian to the ground state of the Fermi sea, the space so created contains only states that are eigenstates of the total spin operator  $S_T = 0$ . This is a direct consequence of the fact that the Hamiltonian commutes with the total spin operator and consequently its application to a  $S_T = 0$  state conserves this eigenvalue of the total spin. Although, this procedure is not capable of reaching the complete Hilbert space of the system, the ground state, our main object of analysis, is contained in it as it is a singlet.

Although the inclusion of states with double occupancy in the correlated  $d$ -level does not introduce any fundamental problem, for simplicity we restrict our study to the infinite Coulomb repulsion  $U$  limit.

Therefore, in order to find the inverse of  $E - H_{22}$  we classify the  $S_T = 0$  sector as follows:

We apply  $H$  to the states  $|\phi_{kd}\rangle$  and considering that double occupancy of the impurity level is prohibited by  $U$ , a new state additional to  $|\phi_1\rangle$  is generated:

$$|\phi_{kK}\rangle = \sum_{\sigma} c_{K\sigma}^{\dagger} d_{\sigma} |\phi_{kd}\rangle. \quad (6)$$

Both,  $|\phi_{kd}\rangle$  and  $|\phi_{kK}\rangle$ , have a single particle–hole excitation from the Fermi sea, where  $k$  ( $K$ ) runs over all wave numbers below (above) the Fermi level. In a similar way, we generate the states that have two particle-hole excitations,

$$|\phi_{kKqd}\rangle = \sum_{\sigma} \frac{d_{\sigma}^{\dagger} c_{q\sigma}}{\sqrt{2}} |\phi_{kK}\rangle, \quad (7)$$

$$|\phi_{kKqQ}\rangle = \sum_{\sigma} c_{Q\sigma}^{\dagger} d_{\sigma} |\phi_{kKqd}\rangle, \quad (8)$$

where  $q$  ( $Q$ ) here as well runs over all wave numbers below (above) the Fermi level. Although, in principle, the wave number  $k$  ( $K$ ) should not be considered because the corresponding state is already unoccupied (occupied), this restriction gives no contribution in the thermodynamical limit, as we discuss below. Rearranging the set of states that form the base of the  $S_T = 0$  sector of  $S_2$  in the following order:  $\{|\phi_{kd}\rangle, |\phi_{kK}\rangle, |\phi_{kKqd}\rangle, |\phi_{kKqQ}\rangle, \dots, |\phi_{k'd}\rangle, |\phi_{k'K}\rangle, \dots\}$ , the matrix of  $E - H_{22}$  can be written as follows:

$$\begin{pmatrix} \epsilon_{kd} & -\frac{V}{\sqrt{N}} & 0 & 0 & \dots & 0 & 0 & \dots \\ -\frac{V}{\sqrt{N}} & \epsilon_{kK} & -\frac{\sqrt{2}V}{\sqrt{N}} & 0 & \dots & 0 & 0 & \dots \\ 0 & -\frac{\sqrt{2}V}{\sqrt{N}} & \epsilon_{kKqd} & -\frac{V}{\sqrt{N}} & \dots & 0 & -\frac{\sqrt{2}V}{\sqrt{N}} & \dots \\ 0 & 0 & -\frac{V}{\sqrt{N}} & \epsilon_{kKqQ} & \dots & 0 & 0 & \dots \\ \dots & \dots & \dots & \dots & \dots & \dots & \dots & \dots \\ \dots & \dots & \dots & \dots & \dots & \dots & \dots & \dots \\ 0 & 0 & 0 & 0 & \dots & \epsilon_{k'd} & -\frac{V}{\sqrt{N}} & \dots \\ 0 & 0 & -\frac{\sqrt{2}V}{\sqrt{N}} & 0 & \dots & -\frac{V}{\sqrt{N}} & \epsilon_{k'K} & \dots \end{pmatrix}$$

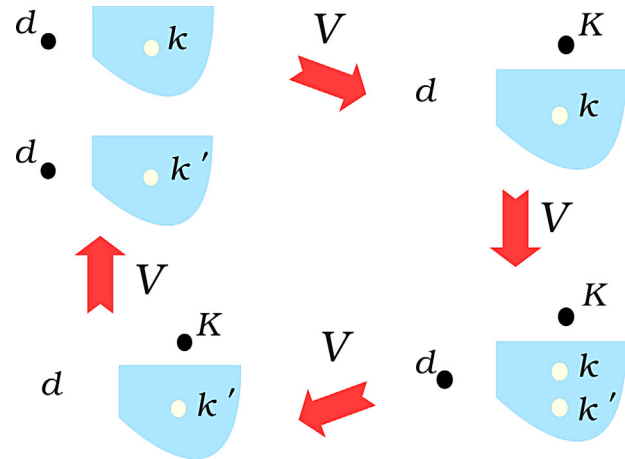


**Figure 1** Scheme of processes that give rise to contributions of  $O(V^4)$  order appearing in Eq. (15), when starting from the state  $|\phi_{kd}\rangle$  and arriving to  $|\phi_{k'd}\rangle$ .

where the energies representing the diagonal terms are

$$\begin{aligned} \epsilon_{kd} &= E - \epsilon_T + \epsilon_k - E_d \\ \epsilon_{kK} &= E - \epsilon_T + \epsilon_k - \epsilon_K \\ \epsilon_{k'd} &= E - \epsilon_T + \epsilon_{k'} - E_d \\ \epsilon_{k'K} &= E - \epsilon_T + \epsilon_{k'} - \epsilon_K \\ \epsilon_{kKqd} &= E - \epsilon_T + \epsilon_k - \epsilon_K + \epsilon_q - E_d \\ \epsilon_{kKqQ} &= E - \epsilon_T + \epsilon_k - \epsilon_K + \epsilon_q - \epsilon_Q \end{aligned} \quad (9)$$

and the dots in the matrix stand for the infinite additional particle–hole excitations.

As usual, the energy  $E$  is calculated relative to the energy of the Fermi sea ground state  $\epsilon_T$ .

In principle, it is possible to obtain all the matrix elements,  $g_{ij}$ , of the resolvent operator  $G = (E - H_{22})^{-1}$ . However, to obtain the energy, given in (5), the calculation only requires the diagonal  $g_{kk}$  and non diagonal  $g_{kk'}$  elements [28]. The scheme, represented in Fig. 1, shows the path connecting two states that are contiguous to  $S_1$  and have different wave numbers, namely  $k$  and  $k'$ . The contribution to the energy of this non-diagonal path that starts from a hole in  $k$  and finishes with a hole in  $k'$  is of the order of  $O(V^4/2D^4)$  times less than the diagonal contribution.

We begin by analyzing, in a first step, only the diagonal contribution to the ground state energy. This term is, as we will show, the most important one in the low-hybridization regimes of the AIM. The matrix element  $g_{kk}$  can be obtained by analyzing the set of infinite equations that give the first column of the matrix  $G$ :

$$\begin{aligned} \epsilon_{kd} g_{kk} - \sum_K \frac{V}{\sqrt{N}} g_{kK} &= 1 \\ -\frac{V}{\sqrt{N}} g_{kk} + \epsilon_{kK} g_{kK} - \sum_{q \neq k} \frac{\sqrt{2}V}{\sqrt{N}} g_{kKq} &= 0 \end{aligned}$$

$$\begin{aligned}
 -\frac{\sqrt{2}V}{\sqrt{N}} g_{kK} + \epsilon_{kKqd} g_{kKq} - \sum_{Q \neq K} \frac{V}{\sqrt{N}} g_{kKqQ} &= 0 \\
 -\frac{V}{\sqrt{N}} g_{kKq} + \epsilon_{kKqQ} g_{kKqQ} &= 0 \\
 \dots & \dots
 \end{aligned} \tag{10}$$

This system of infinite equations can be solved exactly due to the tridiagonal form of the matrix of  $E - H_{22}$ . By eliminating the coefficients, from the last to the first, one can inductively close an expression for the coefficient  $g_{kk}$

$$g_{kk} = \frac{1}{\epsilon_{kd} - \frac{V^2}{N} \sum_K \frac{1}{\epsilon_{kK} - 2\frac{V^2}{N} \sum_q \frac{1}{\epsilon_{kKqd} - \frac{V^2}{N} \sum_Q \frac{1}{\epsilon_{kKqQ} - \dots}} + 2\frac{V^2}{N} \frac{1}{\epsilon_{kkkd} - \dots}} \tag{11}$$

The term in the diagonal energy  $\epsilon_{kkkd}$  (last written term in equation 11) takes into account the contribution coming from the creation of a second hole in the state  $k$ . This term is, in fact, of the order  $1/N$  where  $N$  is the number of sites. It is clear that in the thermodynamical limit,  $N \rightarrow \infty$ , its contribution can be neglected in comparison to the one given by the sum  $\sum_q$ .

This continuous fraction, in a finite system, gives the complete set of energies of the singlet states that satisfy the Schrödinger equation (2). When the thermodynamical limit is taken, each denominator runs over a continuous set of particle-hole excitations. By realizing that this continuous fraction has terms that repeat the structure of previous ones, as for example the term with  $\sum_Q$  in equation 11 that has the same form as the one with  $\sum_K$ , but with the energy shifted, one can re-write this infinite continuous fraction in a simpler form using two auxiliary functions as follows:

$$g_{kk}(E) = \frac{1}{E + \epsilon_k - E_d - F_0(E + \epsilon_k)}, \tag{12}$$

where the function  $F_0$  satisfies the self-consistent functional relationship

$$\begin{aligned}
 F_0(E) &= \frac{V^2}{N} \sum_K \frac{1}{E - \epsilon_K - F_1(E - \epsilon_K)}, \\
 F_1(E) &= 2\frac{V^2}{N} \sum_k \frac{1}{E + \epsilon_k - E_d - F_0(E + \epsilon_k)}. \tag{13}
 \end{aligned}$$

The self-consistent condition represents a non-perturbative treatment to obtain the ground state energy of the many-body Anderson Hamiltonian.

At this point we can make contact with the early solution found by Inagaki [19]. The self-consistent system given by equation in (13) agrees with Eq. (3) of Ref. [19] and represents the core of their treatment, which includes all the

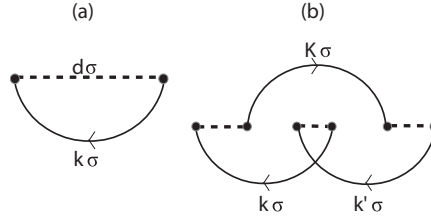


**Figure 2** Diagrams for the perturbation expansion of the ground state energy. (a) and (b) represent the second-order and one example of crossing sixth-order contributions, respectively. The dashed lines represent the electrons at the impurity site while the solid ones represent a conduction electron line to the right and a hole line to the left.

diagrams with non crossing conduction lines as shown if Fig. 2a. As we mention in the introduction, we go beyond this approximation including the non diagonal element  $g_{kk'}$ . This is equivalent to include the crossing diagrams sketched in Fig. 2b that contribute to the ground state energy. The non diagonal elements expressed in terms of the auxiliary functions  $F_0$  and  $F_1$  are given by

$$Q_1(E) = 2\frac{V^2}{N} \sum_{k,k' \neq k} g_{kk'}(E), \tag{14}$$

where the non diagonal element  $g_{kk'}$  is

$$\begin{aligned}
 g_{kk'}(E) &= \frac{V^4}{N^2} \sum_{kk'K} \frac{1}{E + \epsilon_{k'} - E_d - F_0(E + \epsilon_{k'})} \\
 &\times \frac{1}{E + \epsilon_{k'} - \epsilon_K - F_1(E + \epsilon_{k'} - \epsilon_K)} \\
 &\times \frac{1}{E + \epsilon_k + \epsilon_{k'} - \epsilon_K - E_d - F_0(E + \epsilon_k + \epsilon_{k'} - \epsilon_K)} \\
 &\times \frac{1}{E + \epsilon_k - E_d - F_0(E + \epsilon_k)} \\
 &\times \frac{1}{E + \epsilon_k - \epsilon_K - F_1(E + \epsilon_k - \epsilon_K)},
 \end{aligned}$$

which gives in total, taking into account the  $V^2$  in Eq. (14), a contribution of the order  $V^6/N^3$ .

The same kind of crossing diagrams were included in the context of dynamical properties like the impurity Green function [22] within the so-called Post-NCA theory. With this inclusion the Post-NCA approximation, as well as the present contribution, contains the sum of infinite numbers of skeleton diagrams and is exact up to order  $O(1/v^2)$  where  $v$  represents the degeneracy of the impurity level.

When  $F_0$  and  $F_1$  are calculated through an iterative numerical convergent process imposed by the fulfillment of Eq. (13), it is possible to obtain the ground state energy of

the system by the solution of Eq. (5) that can be written as

$$E = F_1(E) + Q_1(E). \quad (15)$$

In what follows we discuss the impurity properties derived by the numerical solution of the Eq. (15).

**3 Numerical results** In this section, we present the numerical results obtained using this formalism. In particular, we analyze the dependence of the ground state energy and the occupancy of the impurity as a function of the energy of the  $d$ -level. Furthermore, we extend the method to include a finite magnetic field and study the magnetization and susceptibility of the impurity.

While the equation (15) gives, in principle, the complete set of eigenvalues in the  $S_T = 0$  space, in what follows we restrict our analysis to the ground state energy.

For this purpose, we transform the discrete self-consistent system (13) into a continuous one,

$$F_0(\omega) = \frac{1}{\pi} \int_0^\infty d\epsilon \frac{\Delta(\epsilon)}{\omega - \epsilon - F_1(\omega - \epsilon)},$$

$$F_1(\omega) = \frac{2}{\pi} \int_{-\infty}^0 d\epsilon \frac{\Delta(\epsilon)}{\omega + \epsilon - E_d - F_0(\omega + \epsilon)}. \quad (16)$$

To solve the self-consistent equations, we consider the hybridization function to be a step function  $\Delta(\epsilon) = \Delta\theta(D - |\epsilon|)$  where  $\Delta = \pi V^2/2D$ , and  $2D$  is the bandwidth,

$$F_0(\omega) = \frac{\Delta}{\pi} \int_{-D+\omega}^\omega \frac{d\epsilon}{\epsilon - F_1(\epsilon)},$$

$$F_1(\omega) = \frac{2\Delta}{\pi} \int_{-D+\omega}^\omega \frac{d\epsilon}{\epsilon - E_d - F_0(\epsilon)}. \quad (17)$$

From now on, we set the hybridization  $\Delta = 1$  as the unit of energy.

It is clear from Eq. (15), that, if the correction  $Q_1$  is not taken into account, the auxiliary function  $F_0$  diverges logarithmically near the ground state energy.

On the other hand, it is easy to verify that if the subspace  $S_1$  is defined by the state

$$|\tilde{\phi}_1\rangle = \frac{1}{\sqrt{2}}(d_\uparrow^\dagger c_{k_F\downarrow}^\dagger - d_\downarrow^\dagger c_{k_F\uparrow}^\dagger) \prod_{k\sigma < k_F} c_{k\sigma}^\dagger |0\rangle, \quad (18)$$

that is an eigenstate of the total  $S_T = 0$  operator, one arrives to exactly the same system of self-consistent equations Eq. (13). The only difference is given by the equation that determines the ground state energy that becomes

$$E - E_d = F_0(E) + Q_0(E), \quad (19)$$

where  $Q_0(E)$  represents the non diagonal contribution and it can be obtained in a similar way used to evaluate  $Q_1(E)$ . As the value of the ground state energy does not depend

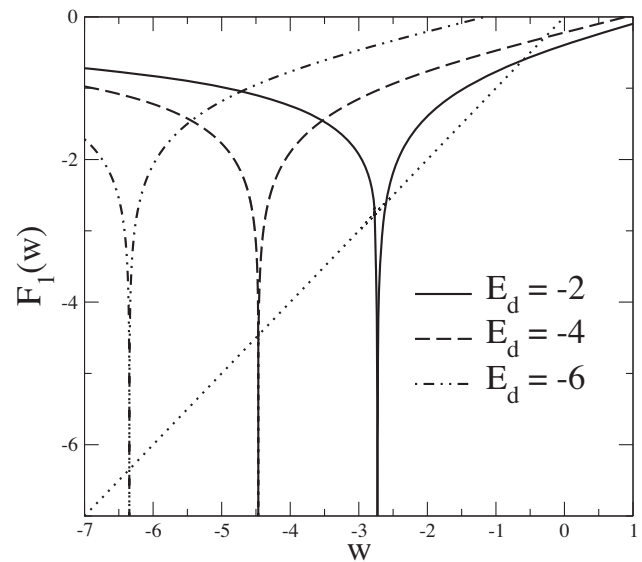


**Figure 3** Converged function  $F_1$  for several values of the  $d$ -level energy. Band width  $D = 10$ . The dotted line represents the linear function  $y = \omega$ . The unit of energy is taken to be  $\Delta = 1$ .

upon the particular form in which the Hilbert space has been partitioned to obtain it, we conclude from Eq. (17) that, if the correction  $Q_0$  is not taken into account, the function  $F_1$  also diverges near the ground state energy.

In Fig. 3, we show the converged function  $F_1$  and a graphical solution of Eq. (15) for several values of the energy of the  $d$ -level. In the first iteration, starting from  $F_0 = 0$ , it is clear that the function  $F_1$  diverges at the value of the impurity energy  $E_d$ . During the self-consistent process, this singular behavior is shifted due to the hybridization.

However, increasing the resolution of the figure in the region where the solution is apparently found, a substructure appears, as can be seen in Fig. 4 showing two extra singularities in the function  $F_1$ . The real solution is contained in this subtle structure, as depicted in the figure. The ground state energy is the one with the lowest energy. The other two solutions cannot be considered as eigenvalues of the Hamiltonian, and they appear as a consequence of the widening of the poles, caused by the introduction of an imaginary part in the denominators of Eq. (16) in order to regularize its behavior.

In order to show the relative magnitude of the correction  $Q_1$  to the ground state energy in Eq. (15), in Fig. 5 we show the ground state energy calculated with and without correction, for a particular value of the hybridization  $\Delta = 1$  and  $D = 10$ . As we have pointed out, the relative importance of the correction increases as the hybridization grows with respect to the other parameters. Moreover, it is important to remark that in the finite  $U$  case, not presented here, the correction is of the order of  $V^4/N^2$ , which increases its relative importance with respect to the  $V^6/N^3$  correction of the infinite  $U$  case, in the low hybridization regimes. We remark that even in this case where the correction is relatively small, it



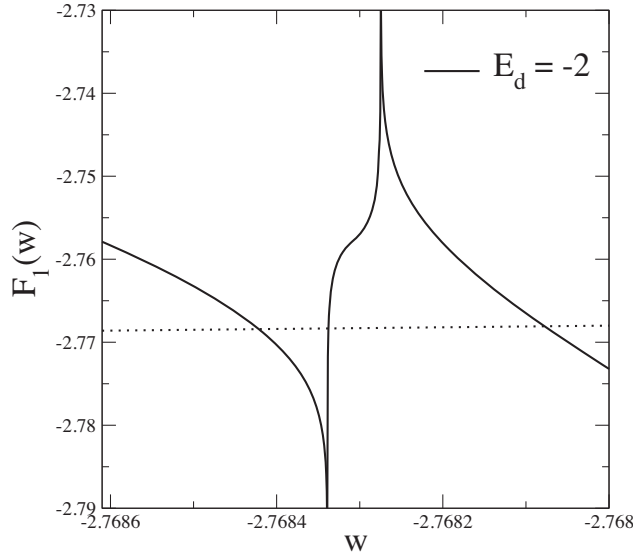


**Figure 4** Amplified region of the converged function  $F_1$  near to the ground state energy. The dotted line represents the linear function  $y = \omega$ . Parameters idem Fig. 3.

can compete with the Kondo temperature. From now on the results presented will include this correction.

The algebraic structure of the formalism we are proposing is essentially the same for a one-body or a many-body problem. As a consequence it is extremely interesting to apply it to obtain the ground state energy of the one-body spinless version of the AIM and to compare the results obtained with the exact Green function solution of this model [29].

The integral self-consistent equations obtained for the spinless system are given by Eq. (13) without the factor 2 in the definition of  $F_1$  due to the inexistence of the spin. In Fig. 6, we compare the results obtained for the ground state energies  $E$  of the interacting version ( $V \neq 0$ ) with respect

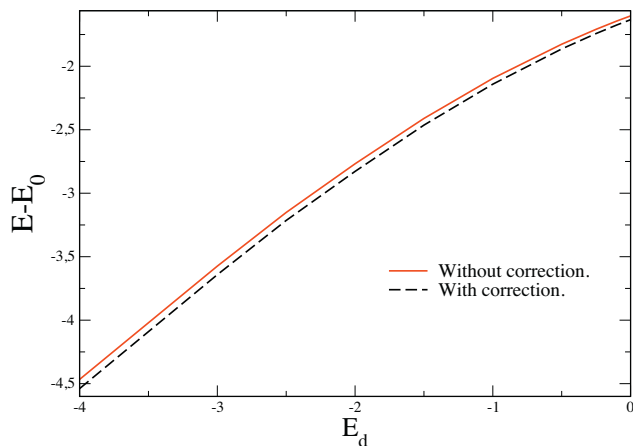


**Figure 5** Ground state energy for  $D = 10$  and  $\Delta = 1$  as a function of the  $d$ -level energy, with and without the correction as calculated with Eq. (14).

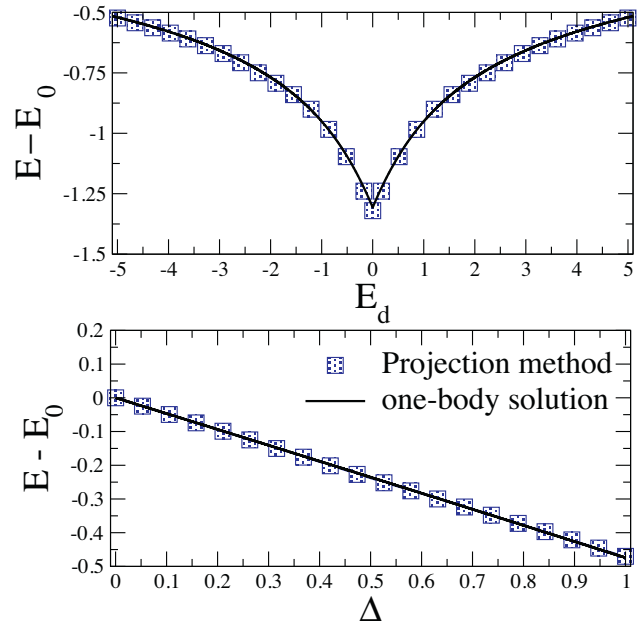


**Figure 6** Top panel: Energy difference between the interacting ( $V \neq 0$ ) and the non-interacting ( $V = 0$ ) spinless AIM as a function of  $E_d$  for  $D = 20$  (top panel) and as a function of the hybridization (bottom panel) for  $D = 10$  and local energy  $E_d = -3$ .

to the non-interacting one  $E_0$  ( $V = 0$ ). The value of  $E_0 = E_d \langle n_d \rangle_0$  naturally depends on the occupation of the isolated impurity given by a step function;  $\langle n_d \rangle_0 = 1$  for  $E_d < 0$  and zero in other case.

An inspection of the figure permits to verify the perfect agreement between the two approaches for all values of  $E_d$ , certifying the correctness of the formalism.

A second relevant test that validates the method is related to the electronic occupation of the impurity  $\langle n_d \rangle$  as a function of its local energy. According to the Hellmann–Feynman theorem, the occupation at the impurity can be extracted from the ground state energy by a simple derivation with respect to the  $d$ -level energy  $E_d$ :

$$\frac{dE}{dE_d} = \left\langle \frac{dH}{dE_d} \right\rangle = \langle n_d \rangle. \quad (20)$$

In Fig. 7, we show the impurity occupation as a function of the impurity level in the limit of infinite bandwidth,  $D \rightarrow \infty$ , and the corresponding ones obtained from the Bethe ansatz approach. The Bethe ansatz expression for the occupancy for infinite Coulomb repulsion can be obtained from Ref. [33].

In Fig. 8, we present the values of the occupancy for a finite bandwidth within our formalism (squares) and, for the same set of parameters, those obtained with the Numerical Renormalization Group (solid line).

From the previous figures we conclude that the results are in excellent agreement with those obtained from exact methods. It is important to stress that various approximated

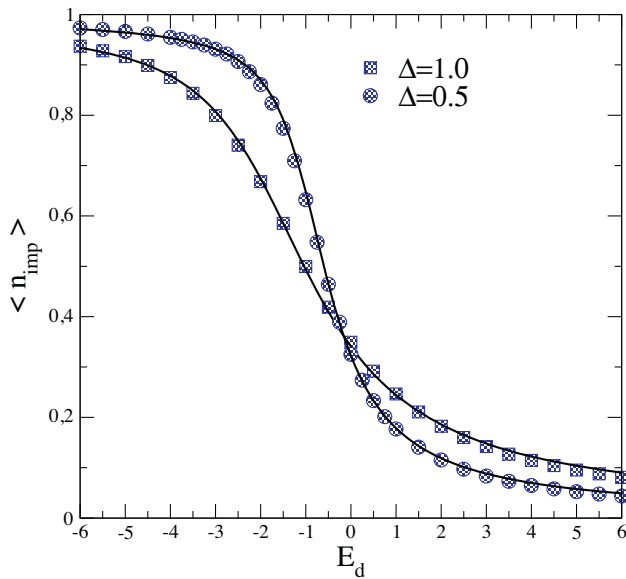


**Figure 7** Occupation of the impurity as a function of the impurity local energy  $E_d$  for two selected values of the hybridization in the limit of the infinite bandwidth,  $D \rightarrow \infty$ . Squares and dots are the results of the present projection method while the solid line stands for the Bethe ansatz solution.

treatments of the AIM do not give reliable results for the occupation. This is the case of the slave-bosons formalism or perturbation theory up to second order in  $V$  neglecting spin flip, see Fig. 2 of Ref. [30]. Our present treatment of the model adequately takes into account, not only the Coulomb repulsion at the  $d$ -level, but also the spin flip processes within a

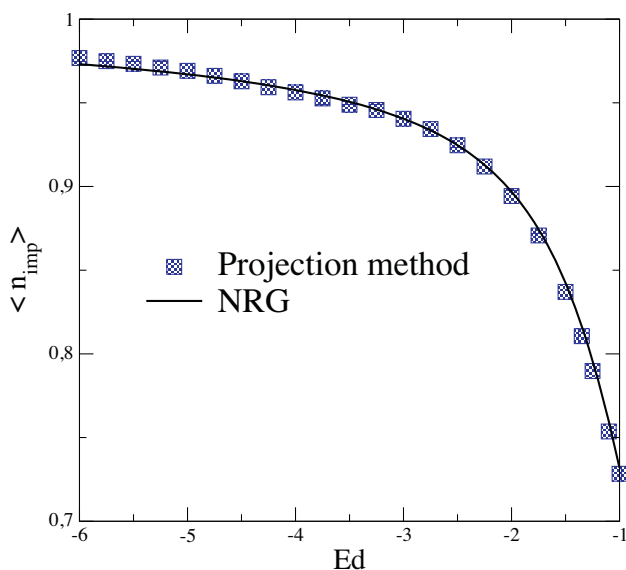


**Figure 8** Occupation of the impurity as a function of the impurity local energy  $E_d$ . Squares represent the present projection method while the solid line stands for the NRG calculations for the same set of parameters,  $D = 10$ .

non-perturbative theory that runs over, in principle, the whole set of particle–hole excitations.

Finally, we add a magnetic field  $B$  to the system and analyze the magnetization and susceptibility of the impurity. Under the effect of a magnetic field, the Hamiltonian becomes

$$H = \sum_{k\uparrow} \epsilon_{k\uparrow} n_{k\uparrow} + \sum_{k\downarrow} \epsilon_{k\downarrow} n_{k\downarrow} + E_{d\uparrow} n_{d\uparrow} + E_{d\downarrow} n_{d\downarrow} + U n_{d\uparrow} n_{d\downarrow} + \sum_{k\sigma} V_k d_{\sigma}^{\dagger} c_{k\sigma} + h.c., \quad (21)$$

where  $\epsilon_{i\uparrow} = \epsilon_i - \mu_B B/2$  and  $\epsilon_{i\downarrow} = \epsilon_i + \mu_B B/2$  and similar expressions for  $E_{d\sigma}$ . In what follows, we use  $\mu_B = 1$ .

The state  $|\phi_{\uparrow}\rangle$  is now a magnetic one due to the increase of the number of conduction electrons with spin up with respect to the spin down ones, while keeping constant the Fermi energy.

The magnetic version of the equation for the energies, Eq. (5), neglecting the non diagonal terms becomes

$$E(B) = \epsilon_{\tau}(B) + \frac{V^2}{N} \sum_{k\uparrow} \langle \phi_{k\uparrow d\uparrow} | \frac{1}{E - H_{22}} | \phi_{k\uparrow d\uparrow} \rangle + \frac{V^2}{N} \sum_{k\downarrow} \langle \phi_{k\downarrow d\downarrow} | \frac{1}{E - H_{22}} | \phi_{k\downarrow d\downarrow} \rangle + O(V^6/N^3), \quad (22)$$

where the state  $|\phi_{k\uparrow d\uparrow}\rangle$  ( $|\phi_{k\downarrow d\downarrow}\rangle$ ) represents the state when a conduction electron with spin  $\uparrow$  (spin  $\downarrow$ ) is promoted to the impurity. Here,  $\epsilon_{\tau}(B)$  stands for the ground state energy of the system without any electron in the impurity level in the presence of the magnetic field  $B$  and  $O(V^6/N^3)$  represent the non diagonal contribution. Following the same procedure sketched previously, we arrive to the spin dependent set of self-consistent integral equations:

$$\begin{aligned} F_{0\uparrow}(\omega) &= \frac{V^2}{N} \sum_{K\uparrow} \frac{1}{\omega - \epsilon_K - F_{1\uparrow}(\omega - \epsilon_K) - F_{1\downarrow}(\omega - \epsilon_K)}, \\ F_{0\downarrow}(\omega) &= \frac{V^2}{N} \sum_{K\downarrow} \frac{1}{\omega - \epsilon_K - F_{1\uparrow}(\omega - \epsilon_K) - F_{1\downarrow}(\omega - \epsilon_K)}, \\ F_{1\uparrow}(\omega) &= \frac{V^2}{N} \sum_{k\uparrow} \frac{1}{\omega + \epsilon_k - E_d + B/2 - F_{0\uparrow}(\omega + \epsilon_k)}, \\ F_{1\downarrow}(\omega) &= \frac{V^2}{N} \sum_{k\downarrow} \frac{1}{\omega + \epsilon_k - E_d - B/2 - F_{0\downarrow}(\omega + \epsilon_k)}. \end{aligned} \quad (23)$$

Finally, the ground state energy can be determined by the solution of the spinless degenerate version of Eq. (15).

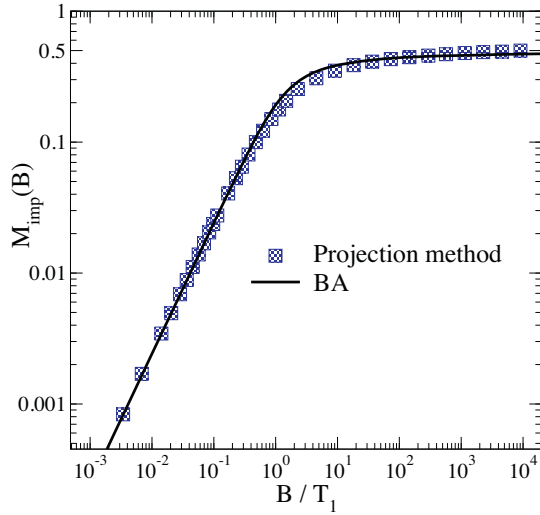


**Figure 9** Comparison of the results obtained by the projection method and the Bethe ansatz for the impurity contribution to the magnetization  $M_{\text{imp}}$  in units of  $g\mu_B$  as a function of  $B/T_1$ . The local level is taken to be  $E_d = -4$ . The scale  $T_1$  is defined in the main text.

In what follows, we focus on the impurity magnetization. According to the usual definition [31], to obtain it we subtract from the total magnetization of the system the magnetization of the isolated Fermi sea. Therefore, the impurity contribution to the magnetization,  $M_{\text{imp}}$ , is given by

$$M_{\text{imp}}(B) = -\frac{\partial}{\partial B}(E(B) - \epsilon_T(B)). \quad (24)$$

In Fig. 9, we show the impurity contribution to the magnetization in units of  $g\mu_B$ , as a function of  $B$ . We chose  $E_d = -4$  to compare our results with the exact Bethe ansatz (BA) results for the Kondo model [32]. The selected value of the energy level  $E_d$  corresponds to the Kondo regime, in which charge fluctuations are frozen, and the Anderson model maps onto the Kondo one.

Following the notation introduced by Andrei in Ref. [32], we define the energy scale  $T_1$ , that characterizes the strong coupling regime [27], from the susceptibility at zero temperature,

$$\chi_{\text{imp}}(B=0) \equiv \frac{\sqrt{2\pi e}}{T_1}. \quad (25)$$

It can be noticed from Fig. 9 that the agreement with the BA is very good. For small values of  $B$  as compared with  $T_1$ , we obtain a linear dependence of the magnetization with respect to the applied field. This agrees with the expected behavior of the Kondo problem indicative of a screened impurity spin. On the other hand, for larger fields, we obtain the characteristic slow asymptotic approach to the value  $g\mu_B/2$  of saturation which also agrees with the well-known logarithmic corrections [32, 7, 34].

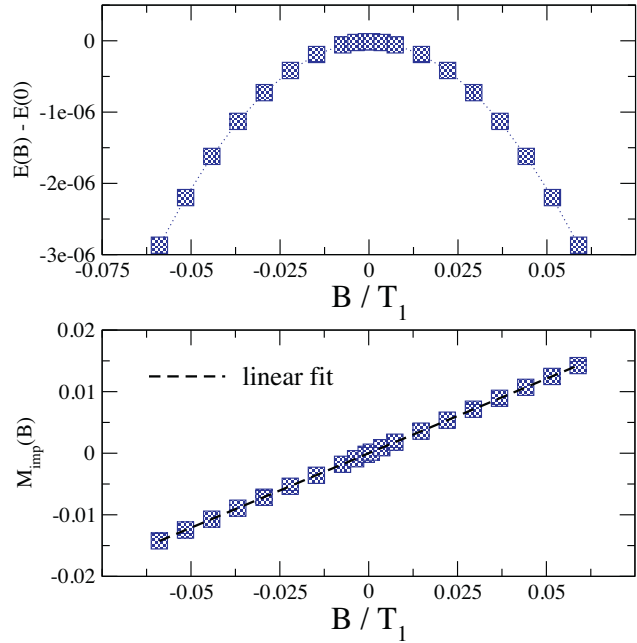


**Figure 10** Energy and magnetization as a function of  $B/T_1$  in the strong coupling regime for  $E_d = -3.5$ . The quadratic and linear shapes respectively are clearly captured. From the inverse of the slope of the magnetization, we obtain the energy scale to be  $T_1 = 0.1070$  in the present case.

At this point, we have to mention that in addition to NRG calculations, the LMA [35] and recent progress in the RPT [36] can also deal with the magnetization of the single impurity Anderson model.

In Fig. 10, we show the energy and magnetization dependence with the applied magnetic field for small values of the field compared with the energy scale  $T_1$ . As was previously mentioned, we obtain a quadratic and linear dependence of the energy and magnetization respectively that agrees with the expected behavior of these magnitudes in the strong coupling regime.

From the definition of the low energy scale  $T_1$ , it is natural [27] to relate it with the usual Kondo scale,  $T_K$ . The dependence of  $T_K$  with the parameters of the Hamiltonian can be extracted, for instance, from the Poor Man's Scaling of the Anderson model [27],

$$T_K = \sqrt{D\Delta} e^{\pi E_d/2\Delta}, \quad (26)$$

that in units of the hybridization energy  $\Delta$  becomes  $T_K = \sqrt{D} e^{\pi E_d/2}$ .

In Fig. 11, we analyze  $\ln(T_1)$  as a function of  $E_d$  for two selected values of the bandwidth  $D$ . As it can be seen, we obtain a linear dependence (dashed lines) with an excellent regression coefficient of the order of 0.99999. The slope of both set of parameters, corresponding to  $D = 10$  and  $D = 20$ , is the same,  $\alpha = 1.545 \pm 0.001$ . It can be noticed that  $\alpha$  differs from  $\pi/2$  by only 2%.



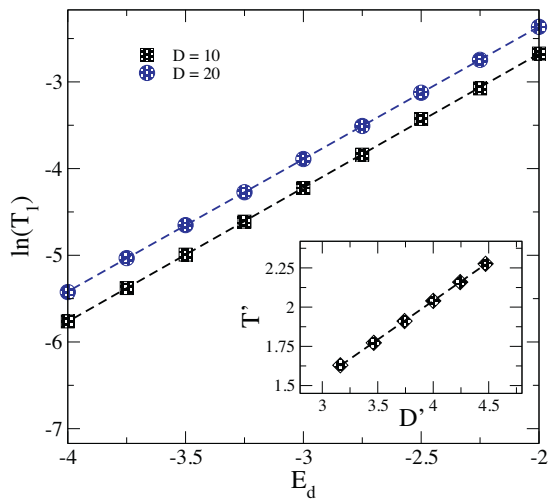


**Figure 11** Evolution of logarithm of  $T_1$  with  $E_d$ , for two different values of the bandwidth  $D$ . The inset shows the scaled energy  $T' = e^{-\pi E_d/2} T_1$  as a function of  $D' = \sqrt{D}$ .

The explicit expression of  $T_1$  can be written as  $T_1 \sim A(D) e^{\pi E_d/2}$ , with a pre-factor that only depends on  $D$ .

The inset of Fig. 11 shows the scaled energy  $T' = e^{-\pi E_d/2} T_1$  as a function of  $D' = \sqrt{D}$ . The dashed line represents a linear regression, again with a great accuracy, with a slope of  $0.484 \pm 0.001$ .

Finally, according to the results obtained we can write the mathematical expression of  $T_1$  as

$$T_1 = \sqrt{8\pi e} T_K, \quad (27)$$

which is a clear indication that the present formalism can deal with the model in its strong coupling regime [27].

**4 Summary and conclusions** We propose an algebraic non-perturbative formalism to solve the Anderson Hamiltonian, which consists in operating in a projected subspace of the total Hilbert space of one many-body function characterized by a ground state Fermi sea of  $N$  particles and an empty impurity. For simplicity we have restricted the discussion to the infinite Coulomb repulsion  $U$ . We were able to show that this treatment, including non-diagonal contributions, corresponds to an extension of previous calculations proposed to obtain the ground state properties of the Hamiltonian [19]. To operate in the projected subspace the Hamiltonian has to be renormalized. A self-consistent functional renormalization of this Hamiltonian permits to obtain the ground state energy and all the static properties of the system; the electronic occupation as a function of the local energy of the impurity, the magnetization, the magnetic susceptibility and the Kondo temperature. We were able to show that the formalism perfectly captures the well-known trends of the model within the whole range of parameters. Conceptually these same ideas can be applied to obtain the Green function of the system and all the dynamical properties. This would require working not only in the  $S = 0$  subspace, some-

thing that in principle can be done with this method. An extension to incorporate more complex system as structures of impurities and magnetic molecules adsorbed on metallic substrate is now been considered. The particular properties of the bulk density of states at the Fermi level neighborhood can be incorporated in a trivial way as it only modifies the function to be integrated in the functional self-consistent processes. This permits to introduce the peculiarities of magnetic impurities adsorbed on a graphene substrate or on any other system described by a highly frequency dependent density of states at the vicinity of the Fermi energy. The use of this formalism to obtain the ground state energy of a periodical system, like the Hubbard model is currently being studied.

**Acknowledgements** This work was partially supported by PIP 00273, of CONICET, and PICT R1776 of the ANPCyT, Argentina. We acknowledge financial support from the Brazilian agencies CNPq and FAPERJ(CNE). The authors are grateful to L. O. Manuel, A. A. Aligia, G. B. Martins and C. A. Büsser for useful discussions and P. Cornaglia for the NRG data.

## References

- [1] P. W. Anderson, *Phys. Rev.* **124**, 41 (1961).
- [2] J. Kondo, *Prog. Theor. Phys.* **32**, 37 (1964).
- [3] A. Georges, G. Kotliar, W. Krauth, and M. Rosenberg, *Rev. Mod. Phys.* **68**, 13 (1996).
- [4] D. Goldhaber-Gordon, H. Shtrikman, D. Mahalu, D. Abusch-Magder, U. Meirav, and M. A. Kastner, *Nature* **391**, 156 (1998).
- [5] M. A. Davidovich, E. V. Anda, C. A. Büsser, and G. Chiappe, *Phys. Rev. B* **65**, 233310 (2002).
- [6] P. B. Wiegmann and A. M. Tselvick, *J. Phys. C, Solid State Phys.* **16**, 2281 (1983).
- [7] A. M. Tselvick and P. B. Wiegmann, *Adv. Phys.* **32**, 453 (1983).
- [8] K. G. Wilson, *Rev. Mod. Phys.* **47**, 773 (1975).
- [9] E. V. Anda, G. Chiappe, C. A. Büsser, M. A. Davidovich, G. B. Martins, F. Heidrich-Meisner, and E. Dagotto, *Phys. Rev. B* **78**, 085308 (2008).
- [10] F. Heidrich-Meisner, A. E. Feiguin, and E. Dagotto, *Phys. Rev. B* **79**, 235336 (2009).
- [11] N. E. Bickers, *Rev. Mod. Phys.* **59**, 845 (1987).
- [12] Th. Pruschke and N. Grewe, *Z. Phys. B, Condens. Matter* **74**, 439 (1989).
- [13] K. Haule, S. Kirchner, J. Kroha, and P. Wölfle, *Phys. Rev. B* **64**, 155111 (2001).
- [14] L. Tosi, P. Roura-Bas, A. M. Llois, and L. O. Manuel, *Phys. Rev. B* **83**, 073301 (2011).
- [15] A. C. Hewson, *Phys. Rev. Lett.* **70**, 4007 (1993).
- [16] A. C. Hewson, *J. Phys.: Condens. Matter* **18**, 1815 (2006).
- [17] D. E. Logan, M. P. Eastwood, and M. A. Tusch, *J. Phys.: Condens. Matter* **10**, 2673 (1998).
- [18] D. E. Logan and M. T. Glossop, *J. Phys.: Condens. Matter* **12**, 985 (2000).
- [19] S. Inagaki, *Prog. Theor. Phys.* **62**, 1441 (1979).
- [20] H. Keiter, J. C. Kimball, *Int. J. Magn.* **1**, 233 (1971).
- [21] Y. Kuramoto, *Z. Phys. B, Condens. Matter* **53**, 37 (1983) and references therein.
- [22] F. B. Anders, *J. Phys.: Condens. Matter* **7**, 2801 (1995).

- [23] S. Streib, A. Isidori, and P. Kopietz, *Phys. Rev. B* **87**, 201107 (2013).
- [24] M. Kinza, J. Ortloff, J. Bauer, and C. Honerkamp, *Phys. Rev. B* **87**, 035111 (2013).
- [25] M. Granath and H. U. R. Strand, *Phys. Rev. B* **86**, 115111 (2012).
- [26] S. Shastry, E. Perepelitsky, and A. C. Hewson, *Phys. Rev. B* **88**, 205108 (2013).
- [27] A. C. Hewson, *The Kondo Problem to Heavy Fermions* (Cambridge University Press, Cambridge, UK, 1993).
- [28] In order to shorten the notation, the index  $d$  is not explicitly included in the matrix elements of  $G$ . So, for instance, the matrix element between the state  $|\phi_{kd}\rangle$  and itself will be noted as  $g_{kk}$ , while that between the state  $|\phi_{kKqd}\rangle$  and itself will be noted as  $g_{kKq}$ , and so on.
- [29] E. Anda, N. Majlis, and D. Grempel, *J. Phys. C* **13**, 2365 (1977).
- [30] P. Roura-Bas, L. Tosi, A. A. Aligia, and P. S. Cornaglia, *Phys. Rev. B* **86**, 165106 (2012).
- [31] R. Bulla, T. A. Costi, and T. Pruschke, *Rev. Mod. Phys.* **80**, 395 (2008).
- [32] N. Andrei, K. Furuya, and J. H. Lowenstein, *Rev. Mod. Phys.* **55**, 331 (1983).
- [33] A. A. Aligia, C. A. Balseiro, and C. R. Proetto, *Phys. Rev. B* **33**, 6476 (1986).
- [34] M. Höck and J. Schnack, *Phys. Rev. B* **87**, 184408 (2013).
- [35] D. E. Logan and N. L. Dickens, *Europhys. Lett.* **54**, 227 (2001).
- [36] K. Edwards, A. C. Hewson, and V. Pandis, *Phys. Rev. B* **87**, 165128 (2013).